Solid Rocket Motor Backflow Analysis For CONTOUR Mishap Investigation

Michael Woronowicz

Swales Aerospace, 5050 Powder Mill Road, Beltsville, Maryland 20705, USA

Abstract. A procedure developed for free molecule modeling of plume backflow from a STAR™ 30BP solid rocket motor is presented for work performed in support of the Comet Nucleus Tour spacecraft mishap investigation. Good general agreement is established with DSMC flowfield results, with interesting deviations developing as the plume backflow approaches the spacecraft surfaces closely, providing insights regarding characteristics of the surface Knudsen layer. Also, investigation of related free expansion results indicate significant discrepancies exist between the rarefied techniques and the continuum results from which their starting surfaces were created. The nature of these differences suggests that convective fluxes to CONTOUR may have been much higher than the rarefied analyses indicated.

INTRODUCTION

On 15 August 2002, the NASA/Johns Hopkins University Applied Physics Laboratory (APL) Comet Nucleus Tour (CONTOUR) spacecraft was destroyed during conclusion of an ATK STAR™ 30BP solid rocket motor (SRM) orbit transfer burn[1]. A NASA Mishap Investigation Board (MIB) was established one week after loss of contact, and under its direction, a number of failure modes were investigated and revisited in greater detail[1]. Without telemetry coverage or direct optical observation to guide them, the MIB was unable to determine the cause of failure indubitably[1]. However, they eventually established the most probable cause through a remarkable sequence of events, beginning with overheating of CONTOUR by backflow from the SRM exhaust plume[1]. The SRM nozzle was nearly immersed within the spacecraft (Fig. 1), allowing nearby surfaces, some of which were bare Aℓ, to be exposed to intolerably high heat fluxes. Such "….overheating may have caused substantial material weakening and structural degradation, which could have led to catastrophic dynamic instability"[1].

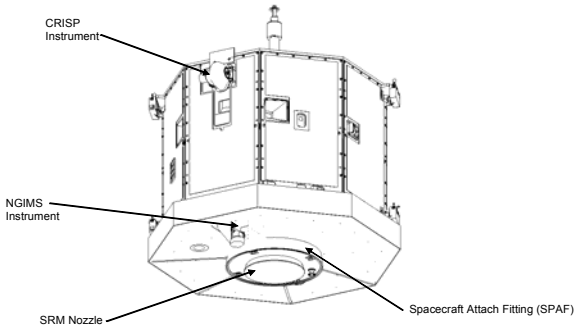

FIGURE 1. Representation of CONTOUR spacecraft, including SRM and SPAF [2].

The MIB decision was guided by sets of analyses describing convective and radiative surface heating due to SRM operations[2-5]. In the final round, one organization used CFD to model SRM product expansion from the nozzle to near field plume development in order to provide a starting surface for rarefied techniques and to establish convective backflow heating estimates from the continuum standpoint[3]. The starting surface provided input conditions for DSMC/DS2V computations as well as a free molecule technique for the same problem[4,5].

CP762, *Rarefied Gas Dynamics: 24th International Symposium,* edited by M. Capitelli

Report Documentation Page

Form Approved
OMB No. 0704-0188

1. REPORT DATE	2. REPORT TYPE	3. DATES COVERED
13 JUL 2005	**N/A**	**-**

4. TITLE AND SUBTITLE	5a. CONTRACT NUMBER
Solid Rocket Motor Backflow Analysis For CONTOUR Mishap Investigation	5b. GRANT NUMBER
	5c. PROGRAM ELEMENT NUMBER
6. AUTHOR(S)	5d. PROJECT NUMBER
	5e. TASK NUMBER
	5f. WORK UNIT NUMBER
7. PERFORMING ORGANIZATION NAME(S) AND ADDRESS(ES) **Swales Aerospace, 5050 Powder Mill Road, Beltsville, Maryland 20705, USA**	8. PERFORMING ORGANIZATION REPORT NUMBER
9. SPONSORING/MONITORING AGENCY NAME(S) AND ADDRESS(ES)	10. SPONSOR/MONITOR'S ACRONYM(S)
	11. SPONSOR/MONITOR'S REPORT NUMBER(S)

12. DISTRIBUTION/AVAILABILITY STATEMENT
Approved for public release, distribution unlimited

13. SUPPLEMENTARY NOTES
See also ADM001792, International Symposium on Rarefied Gas Dynamics (24th) Held in Monopoli (Bari), Italy on 10-16 July 2004. , The original document contains color images.

14. ABSTRACT

15. SUBJECT TERMS

16. SECURITY CLASSIFICATION OF:			17. LIMITATION OF ABSTRACT	18. NUMBER OF PAGES	19a. NAME OF RESPONSIBLE PERSON
a. REPORT	b. ABSTRACT	c. THIS PAGE			
unclassified	**unclassified**	**unclassified**	**UU**	**6**	

Standard Form 298 (Rev. 8-98)
Prescribed by ANSI Std Z39-18

This paper describes the free molecule (FM) analysis[5], an approach which has previously fared well in comparisons with a variety of DSMC simulations and experiments[6,7]. Good general agreement is established with the two-dimensional DSMC/DS2V flowfield, with interesting deviations developing as spacecraft surfaces are approached. These differences illustrate the Knudsen layer's influence in suppressing the excursion of surface-reflected molecules away from the body. Finally, comparisons of related free expansions indicate significant discrepancies exist in the rarefied techniques and the continuum results from which their starting surfaces were created. The nature of these differences suggests that convective fluxes to CONTOUR may have been much higher than the rarefied analyses indicated.

MODEL FORMULATION

A transient solution of the collisionless Boltzmann equation was developed[6,7] to describe the molecular distribution $f(x,t)$ for flow from a point source step function Q_1, where

$$\frac{\partial f}{\partial t} + \boldsymbol{v}\cdot\frac{\partial f}{\partial \boldsymbol{x}} = Q_1; \qquad Q_1 = \frac{2\beta^4}{A_1\pi}\delta(\boldsymbol{x})\dot{m}(t)\left|\boldsymbol{v}\cdot\hat{\boldsymbol{n}}\right|\exp\left(-\beta^2(\boldsymbol{v}-\boldsymbol{u}_e)^2\right), \tag{1}$$
$$A_1 \equiv e^{-s^2\cos^2\phi_e} + \sqrt{\pi}\, s\cos\phi_e\left(1+\operatorname{erf}(s\cos\phi_e)\right).$$

Q_1 represents directed flow from a Lambertian, thermal velocity distribution superimposed on convective exit velocity $\boldsymbol{u}_e$ for mass rate $\dot{m}$, $\beta \equiv 1/\sqrt{2RT}$, and speed ratio $s \equiv \beta u_e$. Normal $\hat{\boldsymbol{n}}$ represents the orientation of a local starting surface element, and $\boldsymbol{v}\cdot\hat{\boldsymbol{n}}$ emphasizes the imposed directional constraint. Generally, $\boldsymbol{u}_e$ is not aligned with $\hat{\boldsymbol{n}}$, with the angle between the two defined by ϕ_e. Local angle ϕ is measured between variable position $\boldsymbol{x}$ (distance r, experiencing local velocity $\boldsymbol{v}$) and $\hat{\boldsymbol{n}}$, and angle θ is measured between $\boldsymbol{u}_e$ and $\boldsymbol{x}$.

The particular solution of Eq. (1) is found using approaches outlined by Bird[8] and Narasimha[9]. The density field generated for a step function in $\dot{m}$ is given by[6,7]

$$\rho(\boldsymbol{x},t) = \frac{\beta\dot{m}\cos\phi}{A_1\pi r^2}e^{w^2-s^2}\left\{(\alpha+w)e^{-z^2} + \left(\frac{1}{2}+w^2\right)\sqrt{\pi}\operatorname{erfc} z\right\}, \tag{2}$$

where $z \equiv \alpha - w$, $\alpha \equiv \beta r/t$, and $w \equiv s\cos\theta$. Solving for successive velocity moments, one finds mass flux $\dot{\Phi}$, incident normal momentum flux $p_\perp$, and incident translational energy flux $\dot{q}_{TR}$:

$$\dot{\Phi}(\boldsymbol{x},t) = \frac{\dot{m}\cos\phi}{A_1\pi r^2}\frac{\boldsymbol{x}}{r}e^{w^2-s^2}\left\{\left(\alpha^2+\alpha w+w^2+1\right)e^{-z^2} + \left(\frac{3}{2}+w^2\right)\sqrt{\pi}\, w\operatorname{erfc} z\right\}, \tag{3}$$

$$\tilde{p}_\perp(\boldsymbol{x},t) = \frac{\dot{m}\cos\phi}{\beta A_1\pi r^2}e^{w^2-s^2}\left\{\left(\alpha^3+\alpha^2 w+\alpha w^2+w^3+\frac{5}{2}w+\frac{3}{2}\alpha\right)e^{-z^2} + \left(\frac{3}{4}+3w^2+w^4\right)\sqrt{\pi}\operatorname{erfc} z\right\}, \tag{4}$$

$$\begin{aligned}\dot{q}_{TR}(\boldsymbol{x},t) = {} & \frac{\dot{m}\cos\phi}{2\beta^2 A_1\pi r^2}\frac{\boldsymbol{x}}{r}\,e^{w^2-s^2} \\ & \times\left\{\left(\alpha^4+\alpha^3 w+\alpha^2 w^2+\alpha w^3+w^4+2\alpha^2+\frac{7}{2}\alpha w+\frac{9}{2}w^2+2\right)e^{-z^2}\right. \\ & \left.+\left(\frac{15}{4}+5w^2+w^4\right)\sqrt{\pi}\, w\operatorname{erfc} z\right\}.\end{aligned} \tag{5}$$

Eq. 4 becomes normal momentum flux $p_\perp$ when multiplied by the dot product r makes with the local normal of the impinged surface. Equations (2)-(4) may be combined to obtain expressions for velocity $\boldsymbol{v}$, translational temperature T_{TR}, and internal energy flux $\dot{q}_{INT}$ for polyatomic molecules having specific heat ratio γ.

$$v(x)=\frac{\dot{\Phi}(x)}{\rho(x)}; \qquad T_{TR}(x)=\frac{1}{3R}\left\{\frac{\tilde{p}_{\perp}(x)}{\rho(x)}-(v(x))^2\right\}; \qquad \dot{q}_{INT}(x)=\left(\frac{5-3\gamma}{\gamma-1}\right)\frac{\dot{\Phi}(x)}{4\beta^2}. \tag{6}$$

Reflected quantities such as normal momentum flux and energy are found by setting $s = 0$, letting $\hat{\boldsymbol{n}}$ represent the local surface element, and assuming the mass flux to a surface element is conserved[8]. The expansion around the nozzle lip into the backflow region may be portrayed by using the near field solution of a continuum code to create a starting surface for a network of FM point sources having locally varying conditions.

PROCEDURE

CONTOUR consisted of an octagonal structure 2.3 m across its apothems on the dustshield end (Fig. 1). The SRM was located within a load-bearing cylinder featuring the spacecraft payload attachment fitting (SPAF). The SPAF cylinder extended 13 cm beyond the dustshield, and the SRM nozzle extended just another 6 cm beyond an annulus of protective insulating blankets. Unprotected metal blanket buttons and an aluminum low-gain antenna (LGA) were exposed to the plume heating. Surface temperature was assumed constant at 333 K.

In early MIB analyses, protruding assemblies were neglected, and the overall geometry was modeled as three stacked, concentric cylinders. Two cases were modeled in the FM investigations; one including the body, and a free expansion. In the former, logic for one set of diffuse surface scattering was added to observe its perturbation on the free expansion, in addition to the perturbation due to physical blocking effects from the structure. The STAR™ 30BP motor consumes 9.2 kg/s of material at a specific impulse of 292 s for about 50 s [10], and SRM gaseous fuel products have been listed in Table 1 below.

Table 1. STAR™ 30BP SRM Model Exhaust Composition at 2450 K[10]

Species	H_2O	H_2	CO	CO_2	$HC\ell$	N_2	$C\ell^-$	H^+
Gaseous Mass Fraction	0.156	0.028	0.300	0.052	0.329	0.130	0.005	< 0.001
Specific Heat Ratio γ	1.18	1.30	1.29	1.16	1.30	1.29	1.65	1.67

Actual SRM exhaust would also contain liquid and solid aluminum compounds. These should be confined to a relatively narrow cone once ejected, and were ignored for the convective backflow analyses.

Exhaust composition is important because as the plume expands, a species separation effect occurs, allowing lightweight constituents to spread more diffusely while heavier ones remain more tightly focused along the plume axis[6,7,12]. Such effects become increasingly important as one moves to higher angles off the plume axis.

RESULTS & DISCUSSION

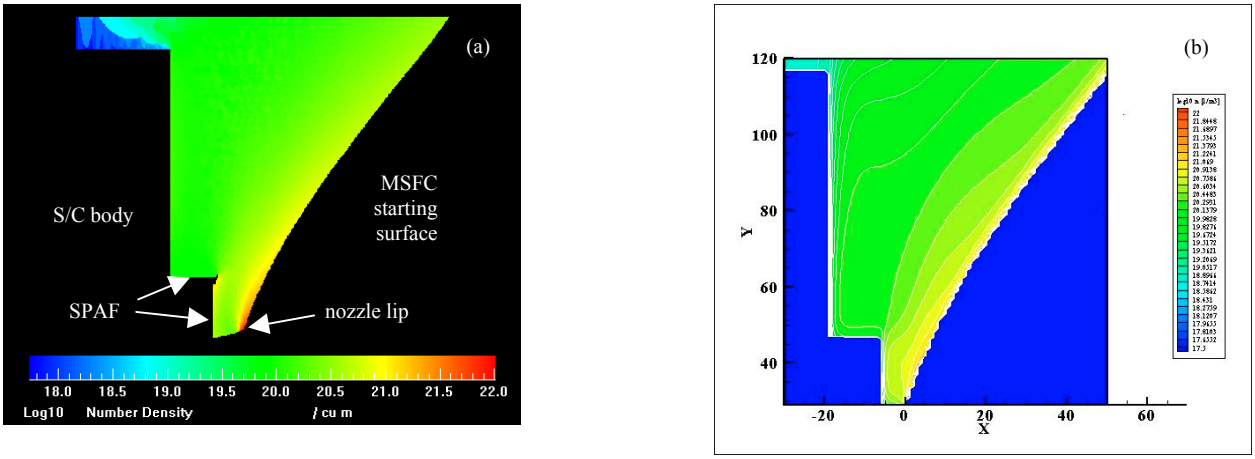

FIGURE 2. Comparison of steady DSMC/DS2V (a) and current FM results (b), logarithmic number density contour maps.

Figure 2 presents a comparison of steady number density (n) contour maps for a radial cross-section on the same logarithmic scale. There is a nice level of agreement overall, considering that for the DSMC case the nozzle lip region was recalculated beginning slightly ahead of the exit plane[4], and more detail has been included in the nozzle and SPAF regions there.

On the other hand, not all differences between the two results can be explained by lower input resolution for the FM case. As spacecraft surfaces are approached, it is clear that n increases in the DSMC case, while it begins to drop for the FM case. Although the author did not have access to raw DSMC simulation output data, careful measurements were made from Fig. 2a above at radial distances of 0.4, 0.6, 0.9, and 1.2 m from the SRM central axis and compared to the FM results (Fig. 3).

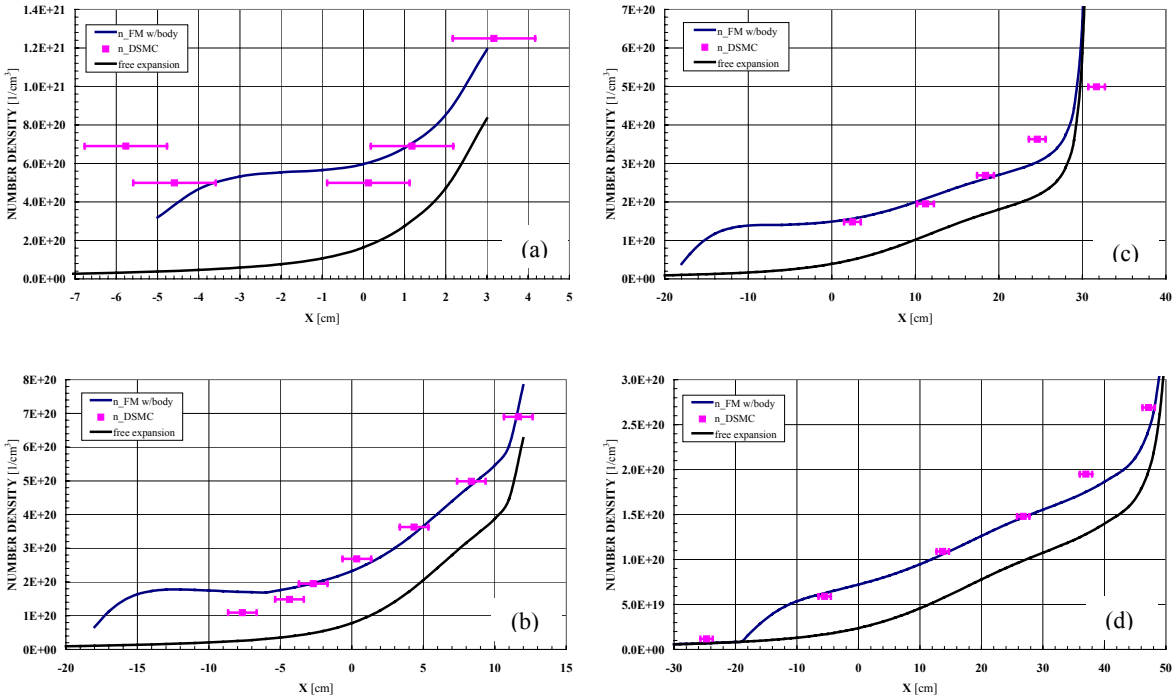

FIGURE 3. Comparison of steady flowfield number density variations for DSMC/DS2V and current FM results at (a) 0.4 m, (b) 0.6 m, (c) 0.9 m, and (d) 1.2 m. CONTOUR spacecraft surfaces located near the vertical axis of each plot (left-hand side), starting surface located along right-hand side. FM free expansion results given by lower curve.

Although it was sometimes too difficult to resolve the precise axial location of individual DSMC contour levels near the body (Figs. 3b & 3c), they qualitatively follow the behavior depicted in Fig. 3a. The rise in density for DSMC results is associated with the radial development of the Knudsen layer across the SPAF closeout ring and the dustshield. Without the interaction between surface-reflected molecules and those approaching directly from the plume starting surface, the FM solution shows no difference between this case and the free expansion (no body) at the body locations.

This absence of FM surface-reflected molecules right at the body location is a consequence of using a diffuse, cosine distribution for the scattered ensemble, which assumes all such molecules must have a component of velocity moving away from the body. Local density is then distributed farther away from the body, giving rise to higher density levels relative to DSMC. These balance out the deficits observed contiguous to the surfaces. Researchers generally refer to the portion of the DSMC profile in Fig. 3a where density increases near the body as the edge of the Knudsen layer. Without a Knudsen layer, FM results show an enhancement of density further afield.

The development of a Knudsen layer in the DSMC solution gives rise to relative variations in heat flux distributions versus the FM results (Fig. 4 below). Both solutions seem to rise from near zero to 0.28 W/cm^2 midway across the SPAF closeout ring, but then the influence of the lip in the DSMC case causes fluxes to increase further, reaching about 0.45 W/cm^2 before the lip is reached. This geometric detail was neglected for FM runs.

Moving radially along the dustshield, both solutions reach a peak net heat transfer of about 0.1 W/cm^2 before declining to about 0.05 W/cm^2 at its outer edge. However, dustshield peak values occur at a lower radius for the FM case. It may be possible to explain this shift either by suggesting higher DSMC cell resolution may be necessary, or

that some sort of local radial convective process is delaying heat flux inputs to the dustshield through the Knudsen layer.

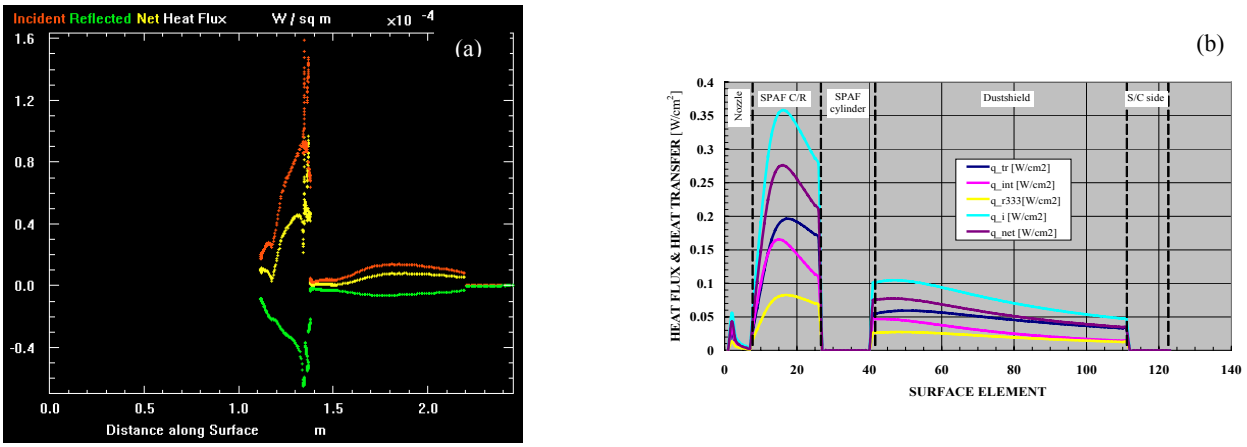

FIGURE 4. Comparison of surface convective heat transfer balance versus running length away from SRM nozzle lip. Net heat transfer presented in yellow for DSMC case (a, middle), purple for FM case (b, second from top).

One alarming discovery made during this investigation regarded free expansion solutions created by the MOC/boundary-layer/CFD approach and the current FM technique (Fig. 5). Somehow, the anticipated exponential decay of mass flux with angle[14] was not observed for FM results using the CFD starting surface, even though the CFD free expansion from which the starting surface was created follows this relationship itself.

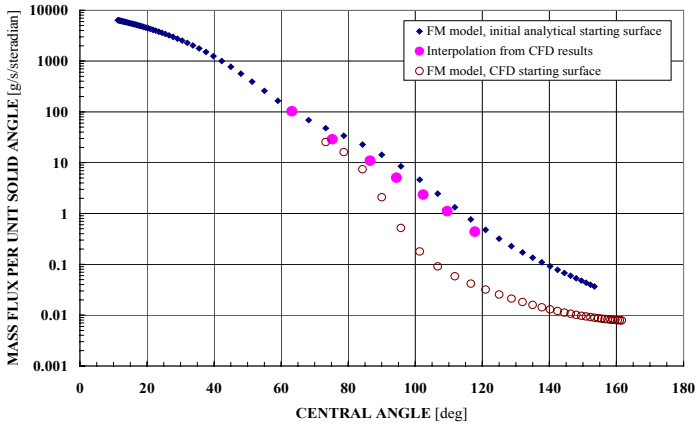

FIGURE 5. Comparison of STAR™ 30BP mass flux angular dependency for steady free expansions, CFD results and FM results using CFD starting surface, performed ~ 1 m off centerline.

No free expansion calculations were performed by the DSMC investigator, but the good agreement between FM and DSMC density contour maps presented in Figs. 2-4 suggests a DSMC free expansion would behave in a fashion similar to the FM result, since fluxes of order higher than density typically behave roughly like a product of density with some suitable power of ultimate velocity. Discrepancies of 10-20× in mass flux would certainly be evident in density comparisons such as Figs. 2 & 3.

Based on these observations, it seems reasonable to assume that the depressed mass flux versus angle relationship at high angles is due to a deficit in density in precisely the same region where SRM backflow impinges on CONTOUR. Such a deficit would yield proportional effects on incident heat fluxes, which is in keeping with early FM work for the CONTOUR MIB using an analytically-based starting surface (Fig. 5)[5]. Based upon these observations, one must consider that actual heat fluxes impinging on CONTOUR in the backflow regime may have been 10-20× higher than what had otherwise been predicted.

Even using the heating rates presented in Fig. 4, other follow-on analyses[2] indicated that structural integrity could have weakened enough during the SRM burn to cause CONTOUR to fail by precipitating dynamic instability.

CONCLUDING REMARKS

A free molecule rocket plume expansion model was used to estimate incident heat fluxes in the backflow regime of an SRM on an actual spacecraft. FM flowfield density results generally compared favorably with DSMC calculations, except as the body was approached closely. In the absence of a Knudsen layer, free molecule results suggest that flowfield behavior near such surfaces is dominated by the gas-surface interaction model employed, and that the flowfield is thus affected over a greater region than what is generally identified with the Knudsen layer.

Attempts to verify an expected mass flux versus angle relationship revealed significant discrepancies exist between FM and DSMC solutions versus the continuum results from which their starting surfaces were created. Further investigation did not determine the cause behind this density deficit, but it is considered possible that actual heat fluxes impinging on CONTOUR's SPAF closeout ring and dustshield may have been even higher than the significant levels presented.

ACKNOWLEDGMENTS

The author gratefully acknowledges support from NASA Contract NAS5-01090, and also wishes to thank the members of the CONTOUR MIB, especially Mr. Craig Tooley, NASA/GSFC, for their support. He also appreciates the efforts of Messrs. Lou Rattenni and Bud Smith for creating the DSMC and CFD solutions discussed herein, and Mr. Frank Giacobbe, Swales Aerospace, for his enthusiasm.

REFERENCES

1. *CONTOUR Mishap Investigation Board Report*, National Aeronautics and Space Administration, Washington, DC, 31 May 2003, <http://www.nasa.gov/pdf/52352main_contour.pdf>.
2. B. Colbert *et al.*, "CONTOUR Spacecraft Base Heating Thermal Analysis Report," MSFC Group Report No. MG-03-446, 18 July 2003, pp. 1-61.
3. S. Smith and P. Anderson, "CONTOUR Spacecraft Base Heating Assessment," MSFC Group Report No. MG-03-173, 20 March 2003, pp. 1-38.
4. L. Rattenni, Jr., "CONTOUR MIB STAR 30BP SRM Convective Plume Heating," presentation package prepared for NASA/GSFC CONTOUR Mishap Investigation Board, 15 April 2003, pp. 1-20.
5. M. Woronowicz, "Further Analysis of STAR 30BP Convective Influences on SPAF Closeout Ring," Swales Aerospace memo to C. Tooley, CONTOUR Mishap Investigation Board, SAI-12-627/MSW-2, 20 May 2003, pp. 1-13.
6. M. Woronowicz, "Development of a Novel Free Molecule Rocket Plume Model," *Rarefied Gas Dynamics 22nd International Symposium*, Sydney, Australia, 9-14 July 2000, American Institute of Physics Conference Proceedings, **585**, Melville, NY, 798-805 (2001).
7. M. Woronowicz, "Further Studies Using a Novel Free Molecule Rocket Plume Model," *Rarefied Gas Dynamics 23rd International Symposium*, Whistler, British Columbia, Canada, 20-25 July 2002, American Institute of Physics Conference Proceedings, **663**, Melville, NY, 588-95 (2003).
8. G. A. Bird, *Molecular Gas Dynamics and the Direct Simulation of Gas Flows*, Clarendon Press, 1994, pp. 77-88.
9. R. Narasimha, "Collisionless expansion of gases into vacuum," *Journal of Fluid Mechanics*, **12**, 294-308 (1962).
10. *Encyclopedia Astronautica*, < http://www.astronautix.com/>.
11. Sobocinski, N.J., "Compliance of the STAR 48B Solid Rocket Motor with PAM-S/ ULYSSES Mission Requirements," Thiokol Corporation Tactical Operations Elkton Division, E260B-87(89), 23 October 1989.
12. G. Koppenwallner, "Species Separation in Rocket Exhaust Plumes and Analytic Plume Flow Models," invited paper, *Rarefied Gas Dynamics 22nd International Symposium*, Sydney, Australia, 9-14 July 2000, American Institute of Physics Conference Proceedings, **585**, Melville, NY, 797 (2001).
13. G. A. Bird, *Molecular Gas Dynamics and the Direct Simulation of Gas Flows*, Clarendon Press, 1994, pp. 360-6.
14. R. Alt, "Bipropellant Engine Plume Contamination Program. Volume 1. Chamber Measurements. Phase 1," Arnold Engineering Development Center, Air Force Systems, Command, AEDC-TR-79-28, Vol. 1, December 1979.